EURASIP Journal on Applied Signal Processing 2002:8, 771–786

Reduced-Rank Chip-Level MMSE Equalization for the 3G CDMA Forward Link with Code-Multiplexed Pilot

Samina Chowdhury
School of Electrical Engineering, Purdue University, West Lafayette, IN 47907-1285, USA
Email: samina@ecn.purdue.edu

Michael D. Zoltowski
School of Electrical Engineering, Purdue University, West Lafayette, IN 47907-1285, USA
Email: mikedz@ecn.purdue.edu

J. Scott Goldstein
SAIC 4001 N. Fairfax Drive, Suite 400, Arlington, VA 22203, USA
Email: sgoldstein@trg1.saic.com

Received 31 July 2001 and in revised form 15 March 2002

This paper deals with synchronous direct-sequence code-division multiple access (CDMA) transmission using orthogonal channel codes in frequency selective multipath, motivated by the forward link in 3G CDMA systems. The chip-level minimum mean square error (MMSE) estimate of the (multiuser) synchronous sum signal transmitted by the base, followed by a correlate and sum, has been shown to perform very well in saturated systems compared to a Rake receiver. In this paper, we present the reduced-rank, chip-level MMSE estimation based on the multistage nested Wiener filter (MSNWF). We show that, for the case of a known channel, only a small number of stages of the MSNWF is needed to achieve near full-rank MSE performance over a practical single-to-noise ratio (SNR) range. This holds true even for an edge-of-cell scenario, where two base stations are contributing near equal-power signals, as well as for the single base station case. We then utilize the code-multiplexed pilot channel to train the MSNWF coefficients and show that adaptive MSNWF operating in a very low rank subspace performs slightly better than full-rank recursive least square (RLS) and significantly better than least mean square (LMS). An important advantage of the MSNWF is that it can be implemented in a lattice structure, which involves significantly less computation than RLS. We also present structured MMSE equalizers that exploit the estimate of the multipath arrival times and the underlying channel structure to project the data vector onto a much lower dimensional subspace. Specifically, due to the sparseness of high-speed CDMA multipath channels, the channel vector lies in the subspace spanned by a small number of columns of the pulse shaping filter convolution matrix. We demonstrate that the performance of these structured low-rank equalizers is much superior to unstructured equalizers in terms of convergence speed and error rates.

Keywords and phrases: CDMA forward link, minimum mean square error equalization, pilot code.

1. INTRODUCTION

Mobile units in current code-division multiple access (CDMA) cellular systems use a Rake receiver, which is a *maximal-ratio combiner* and can be interpreted as a bank of filters matched to the channel that combine the energy from multiple paths [1]. The Rake filter is the optimum (maximum likelihood) demodulator when there is no interference from other users [1]. In IS-95 and the proposed third-generation (3G) systems, orthogonal Walsh-Hadamard codes are used to spread the different users' data symbols on the forward link. At the downlink receiver, after removing the coherent carrier, the signal is multiplied by the synchronized base station long code and then decorrelated with the desired user's spreading code. In a flat fading environment, this will ensure that any interference due to other users in the same cell is eliminated.

However, in urban wireless systems, the fading is often not flat and the orthogonality of the underlying Walsh-Hadamard codes is destroyed at the receiver, resulting in multiple-access interference (MAI) at the receiver. Furthermore, if the multipath delay spread is a significant portion of the symbol period, there will be considerable intersymbol interference (ISI) in addition to the MAI. There are also major interference issues if the mobile unit is near the edge of a cell and is receiving significant out-of-cell transmission, regardless of whether the fading is flat or not. In such environments, the Rake receiver is suboptimal, because it inherently treats MAI as uncorrelated noise. The multipath induced MAI also necessitates very tight power control. When many or all users are active in the cell, the bit error rate (BER) curve of the standard Rake receiver flattens out at higher signal-to-noise ratio (SNR) [2]. Thus, in situations where the number of active users approaches the spreading gain, the Rake receiver does not provide adequate performance.

The maximum likelihood multiuser detector was derived in [3] for the general case, and was shown to have computational complexity that increases exponentially with the number of users. This makes the optimal receiver practically infeasible. Recently, chip-level downlink equalizers have been proposed to significantly increase the capacity of 3G CDMA based high-speed wireless communication links. In the CDMA downlink, for a given user, the signals from all users in the same cell propagate through the same multipath channel, so the multiple-access and interchip interference can be suppressed by linear channel equalization at the chip-level [4]. One advantage of chip-level equalization is that the equalizer coefficients depend only on the downlink multipath channel. In contrast, due to the base station dependent pseudorandom scrambling code, the optimum symbol-level equalizer varies from symbol to symbol, regardless of whether the multipath channel changes or not. Also, the chip-level equalizer is valid for all users, as the coefficients do not depend on the channel short code [5]. Downlink equalization prior to despreading to restore the orthogonality of the different users' signals and hence suppress MAI has been suggested in [2, 4, 5, 6, 7, 8, 9]. Of these, linear zero-forcing (ZF) and minimum mean square error (MMSE) equalizers (proposed by Ghauri and Slock [7] and independently by Krauss et al. [2] and Zoltowski and Krauss [9]) emphasized the multichannel aspect by means of oversampling and/or multiple antennas at the mobile station.

Given a perfect estimate of the common downlink channel, zero-forcing equalization is possible in the noiseless case, regardless of the number of users, provided that sufficient spatio-temporal diversity is available [7]. But in the practical situation of noise in the received signal, the ZF equalizer may suffer from significant noise enhancement. In [2], the sum of the chip sequences from all the users is modeled as an i.i.d. random sequence, resulting in a "simple" chip-level equalizer that does not depend on the (Walsh-Hadamard) channel code, or the base station dependent long code. The equalizer is followed by correlation with the desired user's spreading code and the output, downsampled by the spreading factor, gives the symbol estimate. The resulting chip-level MMSE estimators with perfect channel estimation were shown to outperform both ZF and Rake [2].

References [2, 4, 5, 6, 7, 8, 9] all assumed that the channel statistics and noise power are known at the receiver, hence the performances presented therein represent "upper-bounds" achievable with perfect channel estimation. A blind linear equalization algorithm which equalizes for the common downlink channel was proposed in [10], based on maximizing signal-to-interference plus noise ratio (SINR). Several adaptive versions of chip-level equalizers have been proposed, such as in [11, 12, 13]. In [11], the matched filter for the chip sequence was followed by an adaptive chip decorrelator based on blind linear decorrelation. In [12], the Griffith algorithm was used to update the multiuser chip estimator. However, both receivers were assumed to have perfect channel knowledge. A channel-response minimum-output energy equalizer was proposed in [14], which outperforms Rake for large number of users, provided that the channel estimation error is not significant. Adaptive equalization which requires no knowledge of the channel or the other users' codes was proposed by Frank and Visotsky in [5], where they assumed synchronization with the base station long code and suggested training at chip-level using the code-multiplexed common pilot channel as reference, but no simulation results were presented. This straightforward adaptation does not exploit the orthogonality of the channel codes, and cannot suppress the intracell users due to pseudorandomness of the long code. Hence the SNR in the adaptation is low and the pilot-chip trained equalizer performs as poorly as Rake except at high SNR [13].

For high data rate applications, the multipath delay spread may span numerous chips so that the MMSE equalizer requires computation of a large number of coefficients, and may thus take an unacceptably long time to converge in adaptive implementations. As a result, application of reduced-rank filtering methods in the context of equalization in CDMA has been an active topic of research in recent years. Goldstein et al. [15, 16, 17] first formulated the multistage nested reduced-rank technique for approximating the classical Wiener filter. Their approach uses information from both the covariance matrix and the cross-correlation vector to determine the basis of a lower-dimension subspace that the Wiener filter is constrained to lie within. This method does not require any knowledge of the eigenvectors of the channel covariance matrix, and so involves much less computation than either the principal components (PC) [18] or the cross-spectral components (CS) [19] methods, the two most widely known reduced-rank techniques. A similar approach was developed in [20, 21, 22] where they used an orthonormal auxiliary vector (AV) in conjunction with the matched filter (Rake) to maximize the SINR subject to constraints.

The authors of [23, 24], applied adaptive multistage nested Wiener filter (MSNWF) to the reverse link with asynchronous users, flat fading, and no long code. An important result from their analysis is that the rank D needed to achieve a desired SINR does not scale with system size. Indeed, through extensive supporting simulations, the MSNWF was shown to achieve near optimal SINR performance with a subspace of dimension roughly equal to $D = 8$ or less where the full-rank space was of dimension 128. Another known application of the MSNWF is the cancellation of narrowband and wideband jammers for global positioning system (GPS) employing a power minimization based space-time preprocessor [25, 26].

In this paper, we present reduced-rank, chip-level MMSE estimators based on the MSNWF algorithm. The main goal of this paper is to demonstrate the superior performance of reduced-rank MMSE equalization for the CDMA downlink. We show that, with perfect knowledge of the channel statistics, the MSNWF requires only a small number of stages to achieve near full-rank MMSE performance over a wide range of SNR. We then use a training-based block adaptive algorithm whereby the filter coefficients are adapted *on the symbol-level* using the code-multiplexed pilot channel that carries known symbols, to analyze the performance of the MSNWF when the channel is unknown. The SINR plot shows a convergence speed comparable to full-rank recursive lease square (RLS) and much faster than full-rank least mean square (LMS). Simulated bit error rate curves further illustrate the excellent performance of the MSNWF.

We also present a reduced-rank MMSE equalizer that exploits the structure and sparseness of the multipath channel under high-speed, wideband conditions. In this case, the channel coefficients lie approximately in a subspace associated with only a few columns of the pulse shaping filter convolution matrix. We project the full-rank chip-level MMSE equalizer onto this much lower-rank subspace and illustrate a much better convergence rate than that achieved with an unstructured MMSE equalizer of similar rank.

The results in this paper are for the CDMA forward link with synchronous users, saturated loading, frequency selective fading, long code scrambling and employing two antennas at the mobile receiver. The channel is assumed to be unvarying with time, which is generally true over a short time interval. We also assume that synchronization with the base station long code has been achieved. The rest of the paper is organized as follows. After describing the channel and data models in Section 2, Section 3 derives the chip-level MMSE estimator. Reduced-rank filtering based on the MSNWF is discussed in Section 4, and simulation results obtained for the CDMA downlink is presented in Section 5. Adaptive equalization based on the MSNWF is described in Section 6 along with simulation results. We present the new structured equalizer based on sparse multipath channel in Section 7 and corresponding simulation results in Section 8. Our conclusions are drawn in Section 9.

2. DATA AND CHANNEL MODEL

The channel model is shown in Figure 1. If the transmission is from only one base station, the impulse response for the *i*th antenna channel between the transmitter and receiver (mobile station) is given by

$$h_i(t) = \sum_{k=0}^{N_m-1} h_{c_i}[k]\, p_{rc}(t-\tau_k), \quad i = 1, 2, \tag{1}$$

where $h_{c_i}[k]$ is the time-invariant complex gain associated with the *k*th multipath at the *i*th antenna; $p_{rc}(t)$ is the composite chip waveform (including the matched low-pass filters on the transmit and receive end). The chip waveform is assumed to have a raised cosine spectrum. And N_m is the total number of delayed paths, that is, multipath arrivals, some of which may have zero or negligible power, so that the channel impulse response is sparse.

The transmitted "sum" signal may be described as

$$s[n] = c_{bs}[n] \sum_{j=1}^{N_u} \sum_{m=0}^{N_s-1} b_j[m]\, c_j[n - N_c m], \tag{2}$$

where $c_{bs}[n]$ is the base station dependent long code, $b_j[m]$ is the bit/symbol sequence of the *j*th user, $c_j[n]$ is the *j*th user's channel (short) code of length N_c, N_u is the total number of active users, N_s is the number of bit/symbols transmitted during a given time window.

The signal received at the *i*th antenna (after convolving with a matched filter having a square-root raised cosine impulse response) is given by

$$x_i(t) = \sum_n s[n]\, h_i(t - nT_c) + \eta_i(t), \quad i = 1, 2, \tag{3}$$

where T_c is the duration of one chip and $\eta_i(t)$ is a noise process assumed white and Gaussian prior to coloration by the receiver chip-pulse matched filter.

2.1. Edge of cell/soft handoff

We consider the interference problem when the desired user is at the edge of a cell so that the total received signal at the mobile station is the sum of the contributions from two base stations, plus noise

$$x_i(t) = x_i^{(1)}(t) + x_i^{(2)}(t) + \eta_i(t), \quad i = 1, 2 \text{ antennas at receiver}, \tag{4}$$

where $x_i^{(l)}(t)$ denotes the signal received at the *i*th antenna due to transmission from the *l*th base station, and $x_i(t)$ denotes the total received signal at the *i*th antenna.

At each antenna, we oversample the signal $x_i(t)$ to obtain $r_{1i}[n] = x_i(nT_c)$ and $r_{2i}[n] = x_i(T_c/2 + nT_c)$.

In the *soft handoff* mode, the desired user's data is transmitted simultaneously from the two base stations. At the receiver, two equalizers are designed, one for each base station. The output of each of the two chip-level equalizers is correlated with the desired user's channel code times the corresponding base station's long code. These two symbol estimates are averaged to get the symbol estimate for the soft handoff mode. The block-diagram for the chip-level MMSE equalizer employing soft handoff is shown in Figure 2. In the *normal* mode, the second base station is treated as interference.

3. CHIP-LEVEL MMSE ESTIMATOR

The chip-level MMSE equalizer is designed to minimize the MSE between the multiuser synchronous sum signal, $s[n]$, and the sum of the equalizer outputs, as depicted in Figures 1 and 2. Given the orthogonality of the channel codes, an estimate of the symbol, $\hat{b}_j[m]$, can be obtained via a correlate and sum with c_j and c_{bs} at the output of the chip-level MMSE equalizer.

Equation (4) can be written more compactly in vector form as

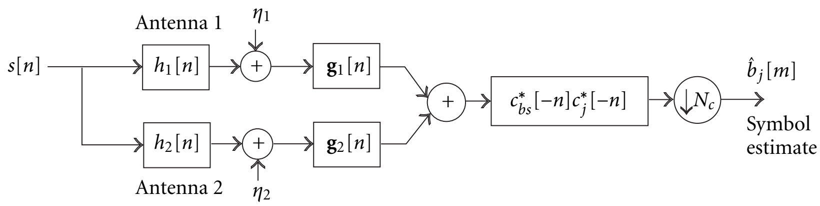

Figure 1: Chip-level MMSE equalization for CDMA downlink with one base station.

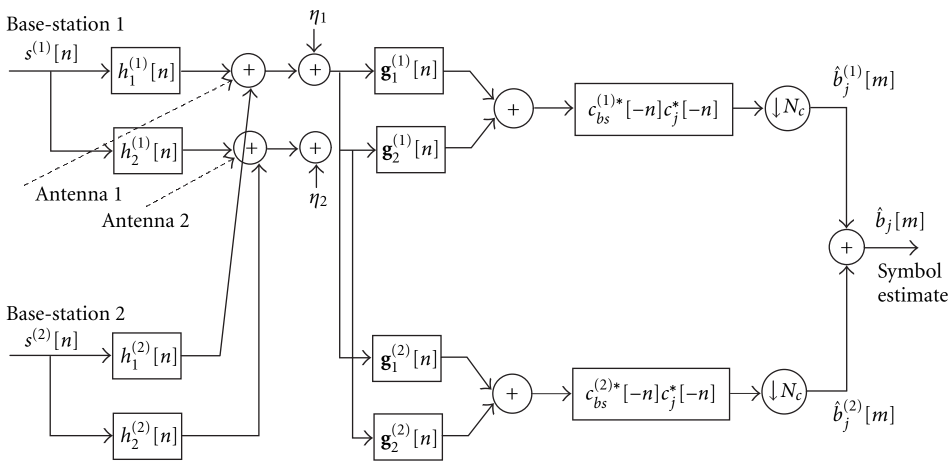

Figure 2: Chip-level MMSE equalization for CDMA downlink, two base stations, soft handoff.

$$\begin{aligned}\mathbf{x}[n] &= \mathbf{H}^{(1)}\mathbf{s}^{(1)}[n] + \mathbf{H}^{(2)}\mathbf{s}^{(2)}[n] + \boldsymbol{\eta}[n] \\ &= \mathcal{H}\mathbf{s}[n] + \boldsymbol{\eta}[n],\end{aligned} \tag{5}$$

where $\mathbf{H}^{(l)}$ is the $2N_g \times (L + N_g - 1)$ channel convolution matrix (N_g is the length of the equalizer, and L is the length of the channel in chips.), comprised of

$$\mathbf{H}^{(l)} = \begin{bmatrix} \mathbf{H}_1^{(l)} \\ \mathbf{H}_2^{(l)} \end{bmatrix}, \tag{6}$$

where

$$\mathbf{H}_i^{(l)} = \begin{bmatrix} h_i^{(l)}[0] & 0 & \cdots & 0 \\ h_i^{(l)}[1] & h_i^{(l)}[0] & \cdots & 0 \\ \vdots & \ddots & \ddots & \ddots \\ h_i^{(l)}[L-1] & h_i^{(l)}[L-2] & \cdots & \cdots \\ \vdots & \ddots & \ddots & \ddots \\ 0 & 0 & h_i^{(l)}[L-1] & \cdots \end{bmatrix}^T. \tag{7}$$

$\mathcal{H}$ is the composite channel convolution matrix $\mathcal{H} = [\mathbf{H}^{(1)} \quad \mathbf{H}^{(2)}]$. And $\mathbf{s}^{(l)}[n]$ is an $(L+N_g-1)$ vector of the transmitted signal, with the superscript denoting the corresponding base station.

The corresponding formulae for only one transmitting base station can be found by simply removing the term involving $\mathbf{H}^{(2)}$ from (5).

Krauss et al. [2] made some simplifying assumptions to derive a chip-level MMSE equalizer that can be easily implemented. The sequence values for the multiuser sum signal are assumed to be i.i.d. random variables. Otherwise, the covariance matrix of the sum signal $\mathbf{s}[n]$ is a complicated expression involving the Walsh-Hadamard spreading codes that vary from index to index. The i.i.d. assumption is valid if the (long) scrambling code is viewed as a random i.i.d. sequence and/or all users are active with equal power. With this assumption, the covariance matrix of the signal is $E\{\mathbf{s}[n]^H\mathbf{s}[n]\} = \sigma_s^2\mathbf{I}$, and the MMSE equalizer was shown to be

$$\mathbf{g}_c^{(l)} = \left\{\sigma_s^2\mathcal{H}\mathcal{H}^H + \mathcal{R}_{\eta\eta}\right\}^{-1}\mathbf{H}^{(l)}\boldsymbol{\delta}_{D_c}, \tag{8}$$

where $\boldsymbol{\delta}_{D_c}$ is a column vector of all zeros except 1 in the (D_c+1)th position, D_c is the combined delay of the equalizer and channel, σ_s^2 is the signal power, and $\mathcal{R}_{\eta\eta} = E[\boldsymbol{\eta}^H[n]\boldsymbol{\eta}[n]]$. In [2] and Section 5 of this paper, the delay D_c, $0 \le D_c \le (N_g + L - 2)$, that yields the smallest MMSE is calculated using the actual channel statistics and that D_c is used in the simulations.

Equation (8) has the form of the well-known Wiener-Hopf solution,

$$\mathbf{w} = \mathbf{R}_{xx}^{-1}\mathbf{r}_{dx}, \tag{9}$$

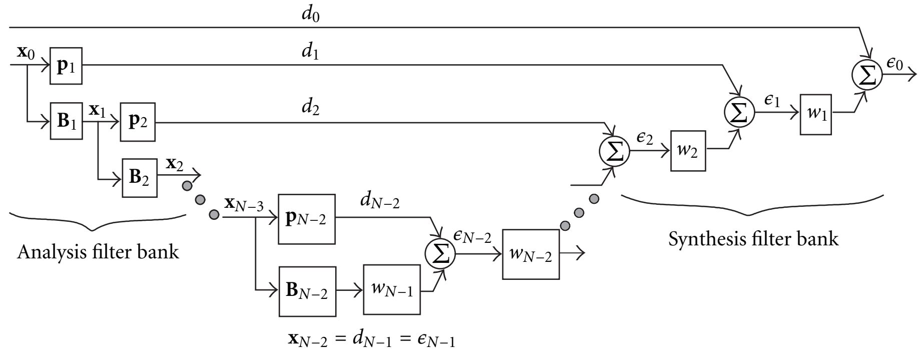

FIGURE 3: Structure of successive stages of the multistage nested Weiner filter.

where $\mathbf{R}_{xx}$ is the channel covariance matrix and $\mathbf{r}_{dx}$ is the cross-correlation vector.

In [2, 27], the authors showed that the MMSE significantly outperforms the Rake receiver, especially when a large number of channel codes are active relative to the spreading factor. The difference is more pronounced when soft handoff is unavailable.

4. REDUCED RANK FILTERING

In general, the length of an MMSE equalizer should be at least equal to the channel length to achieve the desired performance, and longer equalizers yield better error rates [28]. Hence equalizers in the high-speed CDMA downlink will by necessity span many chips in length with a corresponding large number of degrees of freedom. In order to reduce the number of filter coefficients to be estimated, the received signal vector may be projected onto a lower dimensional subspace, and the Wiener filter given by (9) constrained to lie in this subspace. This increases the speed of convergence dramatically for adaptive methods, if the subspace is chosen properly. But the overall MMSE for the reduced-rank filter may be higher than the MMSE for the full-rank filter. The most widely known reduced rank techniques in signal processing are the principal components method [18] and the cross-spectral methods [19], both based on eigendecomposition of the channel covariance matrix.

4.1. *Multistage nested Wiener filter*

Goldstein et al. [15, 16, 17] first formulated the MSNWF, which uses information from the channel covariance matrix, $\mathbf{R}_{xx}$, and cross-correlation vector, $\mathbf{r}_{dx}$, to determine the bases of the lower-dimension that $\mathbf{w}$ is constrained to lie within. The structure of the MSNWF is depicted in Figure 3. At each stage, a rank-one basis is selected based on maximal correlation between the desired signal, d_0, and the observed signal $\mathbf{x}_0[n]$. The observed vector process is decomposed by a sequence of nested filters $\mathbf{p}_1, \mathbf{p}_2, \dots, \mathbf{p}_D$, where D is the order of the filter,

$$\mathbf{p}_k = \frac{E[\mathbf{x}_{k-1}\, d_{k-1}^*]}{||E[\mathbf{x}_{k-1}\, d_{k-1}^*]||}, \tag{10}$$

and $d_k = \mathbf{p}_k^H \mathbf{x}_{k-1}$.

- *Initialization:*
  $\mathbf{c}_1 = \mathbf{r}_{dx} = E[\mathbf{x}_0 d_0^*]$, $\delta_1 = \sqrt{\mathbf{r}_{dx}^H \mathbf{r}_{dx}}$,
- *Forward recursion:*
  For $k = 1, 2, \dots N-1$ Do
  (1) $\mathbf{p}_k = \mathbf{c}_k/\delta_k$,
  (2) $\mathbf{B}_k = \text{null}(\mathbf{p}_k)$,
  (3) $d_k = \mathbf{p}_k^H \mathbf{x}_{k-1}$,
  (4) $\mathbf{x}_k = \mathbf{B}_k \mathbf{x}_{k-1}$,
  (5) $\mathbf{c}_{k+1} = E[\mathbf{x}_k d_k^*]$,
  (6) $\delta_{k+1} = \sqrt{\mathbf{c}_{k+1}^H \mathbf{c}_{k+1}}$,
- End
  $\mathbf{x}_{N-1} = d_N = \epsilon_N$,
- *Backward recursion:*
  $\xi_N = E[|\mathbf{x}_{N-1}|^2]$, $\delta_N = E[\mathbf{x}_{N-1}\, d_{N-1}^*]$, $w_N = \delta_N/\xi_N$,
- For $k = N-1, \dots, 2, 1$ Do
  (1) $\epsilon_k = d_k - w_{k+1}\epsilon_{k+1}$,
  (2) $\xi_k = \sigma_{d_k}^2 - \delta_{k+1}^2/\xi_{k+1}$,
  (3) $w_k = \delta_k/\xi_k$,
- End

ALGORITHM 1: Basic MSNWF algorithm.

The input process to the $(k+1)$th stage is $\mathbf{x}_k[n] = \mathbf{B}_k \mathbf{x}_{k-1}[n]$, where $\mathbf{B}_k$ is a *blocking* matrix such that $\mathbf{B}_k \mathbf{p}_k = 0$.

The outputs of the various stages are linearly combined via the *scalar* weights, $w_1, w_2, \dots, w_{D-1}$, chosen so that the mean square error at each stage is minimized. If the decomposition is carried out for the full N stages, then the multistage nested filter is exactly equivalent to the full-rank classical Wiener filter [15]. The filter-bank structure whitens the error residue at each stage, and compresses the colored portion of the observed data subspace and hence, it is optimal in terms of reducing the MSE for a given rank. The MSNWF does not require any eigen decomposition or inversion of the covariance matrix, and so represents a significant reduction in complexity over the full-rank Wiener solution and other reduced-rank techniques. This is very important for practical implementations, particularly if the rank one decomposition can be stopped after a few stages. The basic algorithm, based on [15] is listed in Algorithm 1.

It is straightforward to see that the "desired" signal at

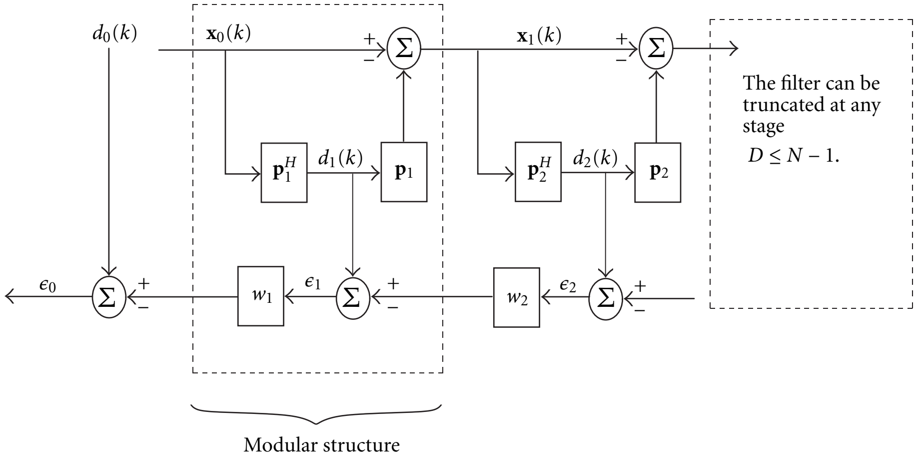

FIGURE 4: MSNWF as a lattice filter.

each stage, $d_k[n]$ is the output of a length N filter,

$$\mathbf{c}_k = \left(\prod_{i=1}^{k-1} \mathbf{B}_i^H\right)\mathbf{p}_k. \tag{11}$$

A notable feature is that the first filter is orthogonal to filters of all the following stages, that is,

$$\mathbf{c}_k^H \mathbf{c}_1 = \delta_{k1}, \quad k = 1, 2, \ldots, N, \tag{12}$$

δ_{ki} denotes the Kronecker delta function, which is 1 for $k = i$, and 0 otherwise. However, the filters $\mathbf{h}_k$, $k = 2, 3, \ldots, N$, are not mutually orthogonal in general. The operation of the analysis filter-bank can be combined into a $D \times N$ transfer matrix, given by

$$\mathbf{T}_D = \begin{bmatrix} \mathbf{p}_1^H \\ \mathbf{p}_2^H \mathbf{B}_1 \\ \vdots \\ \mathbf{p}_D^H \prod_{k=D-1}^{1} \mathbf{B}_k \end{bmatrix} = \begin{bmatrix} \mathbf{c}_1^H \\ \mathbf{c}_2^H \\ \vdots \\ \mathbf{c}_D^H \end{bmatrix}. \tag{13}$$

The orthogonal decomposition ensures that the reduced dimension $D \times D$ correlation matrix $\mathbf{T}_D \mathbf{R}_{xx} \mathbf{T}_D^H$ is tridiagonal [15].

Honig and Xiao [24] first proposed choosing a projection matrix on to the subspace orthogonal to $\mathbf{p}_k$ as the blocking matrix at each stage, hence retaining the length N of the filter and the "observed signal" $\mathbf{x}_k[n]$. With this choice for the blocking matrix, $\mathbf{T}_D = [\mathbf{p}_1 \ \mathbf{p}_2 \ \cdots \ \mathbf{p}_D]$ forms an orthonormal basis for the reduced dimension subspace. Moreover, $\mathbf{w}$ is constrained to lie in the Krylov subspace spanned by $\{\mathbf{r}_{dx}, \mathbf{R}_{xx}\mathbf{r}_{dx}, \mathbf{R}_{xx}^2\mathbf{r}_{dx}, \ldots \mathbf{R}_{xx}^{D-1}\mathbf{r}_{dx}\}$ [24]. In this case,

$$\mathbf{p}_{k+1} = \frac{(\mathbf{I} - \mathbf{p}_k\mathbf{p}_k^H)\mathbf{R}_{k-1}\mathbf{p}_k}{\|(\mathbf{I} - \mathbf{p}_k\mathbf{p}_k^H)\mathbf{R}_{k-1}\mathbf{p}_k\|}, \tag{14}$$

where

$$\mathbf{R}_k = (\mathbf{I} - \mathbf{p}_k\mathbf{p}_k^H)\mathbf{R}_{k-1}(\mathbf{I} - \mathbf{p}_k\mathbf{p}_k^H), \quad \text{for } k = 1, 2, \ldots, D, \tag{15}$$

$\mathbf{p}_1 = \mathbf{r}_{dx}$, $\mathbf{R}_0 = \mathbf{R}_{xx}$.

Joham and Zoltowski [29] proved that this choice of the blocking matrix, that is, $\mathbf{B}_k = \mathbf{I} - \mathbf{p}_k\mathbf{p}_k^H$, is optimum in terms of maximizing the correlation between the scalar signals $d_k[n]$ and $d_{k-1}[n]$ at each stage. They developed a covariance-level *order recursive* form of the MSNWF working within the Krylov subspace, in which the backwards recursion coefficients and hence the weight vector and the mean square error, may be updated at each stage via a simple recursion.

4.2. Lattice structure of the MSNWF

The *blocking matrix* is a very useful concept to develop and analyze the performance of the MSNWF, but in practice, there is no need to calculate or store these $N \times N$ matrices. A new reduced-complexity implementation was presented by Ricks and Goldstein in [30] based on the following substitution: at the kth stage

$$\begin{aligned} d_k[n] &= \mathbf{p}_k^H \mathbf{x}_{k-1}[n], \\ \mathbf{x}_k[n] &= \mathbf{B}_k \mathbf{x}_{k-1}[n] \\ &= [\mathbf{I} - \mathbf{p}_k^H \mathbf{p}_k]\mathbf{x}_{k-1}[n] \\ &= \mathbf{x}_{k-1}[n] - d_k[n]\mathbf{p}_k. \end{aligned} \tag{16}$$

This leads to the "lattice-type" structure for a D-stage MSNWF, as shown in Figure 4. This architecture has the benefit of being modular and scalable for hardware implementation, as well as being computationally more efficient than the structure depicted in Figure 3.

5. APPLICATION OF MSNWF TO CDMA DOWNLINK

Our first set of results solves for chip-level MMSE equalization based on (8) when only one base station is transmitting

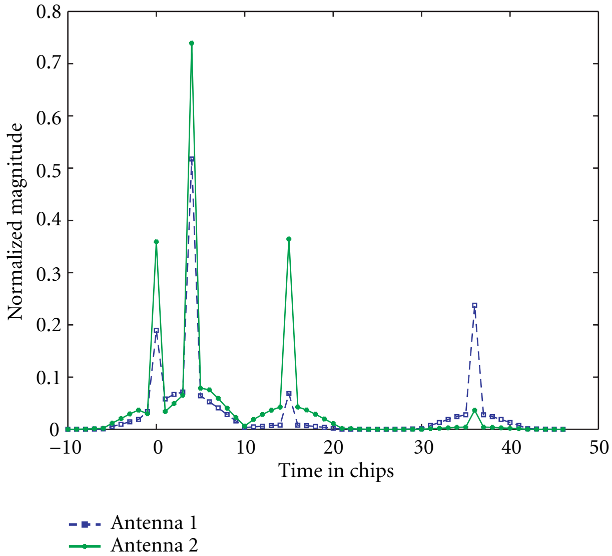

FIGURE 5: Typical channel impulse response for simulated model.

and finds the "ideal" MSNWF solution after various stages, assuming that $\mathbf{R}_{xx}$ and $\mathbf{r}_{dx}$ are known (perfect channel estimation). The same simulations are also done for the edge of cell situation, when two base stations of equal power are received at the mobile-station and the receiver uses soft handoff.

A wideband CDMA forward link was simulated similar to one of the options in the US CDMA2000 proposal. The chip rate was 3.6864 MHz ($T_c = 0.27\,\mu$s), 3 times that of IS-95. Simulations were performed for a *saturated cell*, that is, all possible 64-channel codes are active, and all users have *equal* power. The spreading factor was $N_c = 64$ chips per bit. The data symbols were BPSK, and spread with one of 64 Walsh-Hadamard codes. The signals were summed synchronously and then multiplied with a QPSK scrambling code of length 32678, similar to the IS-95 standard.

The channels were modeled to have four equal-power multipaths, uniformly distributed within a delay spread of 10 microseconds (corresponding to about 37 chips). The multipath coefficients are complex normal, independent random variables. The arrival times at antenna 1 and 2 are the same, but the multipath coefficients are independent. Figure 5 shows a typical channel's impulse response with tails, sampled at the chip rate.

In the two-base station case, the maximum delay spread of the downlink channel from the second base station is also 10 microseconds, with 4 dominant multipaths arrivals at random. The channels are scaled so that the total energy from each of the two base stations is equal at the receiver. Specifically,

$$\sum_{m=1}^{M} E\left\{\left|x_m^{(1)}[n]\right|^2\right\} = \sum_{m=1}^{M} E\left\{\left|x_m^{(2)}[n]\right|^2\right\}. \tag{17}$$

SNR is defined to be the ratio of the sum of the average power of the received signals over all the channels, to the average noise power, after chip-matched filtering. Since the spreading factor (number of chips per symbol) is equal to the number of users, and each user contributes the same amount of power, this chip signal SNR is equal to the postcorrelation (or despread) SNR per user per symbol. The curves were generated by averaging 100 or more different channels. Note that the abscissa in the graphs is the postcorrelation SNR for *each* user, which includes a processing gain of $10\log(64) \approx 18$ dB.

Figure 6 plots the mean square error for the different reduced-rank methods as a function of the subspace dimension, D. The channel statistics and noise power are assumed to be known. In the single base station case, Figure 6a, the dimension of the full space is 114 (the equalizer length is 57 at each of the 2 antennas, as multipath delay spread is 37 chips and the chip pulse waveform is cut off after 5 chips at both ends). The MSE for MSNWF is seen to drop dramatically with D, and achieves the performance of the full-rank Wiener filter at dimension approximately 7! In contrast, the principal components method takes longer than twice the delay spread, and the cross-spectral method does only slightly better.

Figure 7a displays the BER curves obtained with the MSNWF for different sizes of the reduced-dimension subspace. For comparison, the BER for a conventional Rake and full-rank chip-level MMSE equalizer are also shown. The channel statistics are assumed to be known perfectly, so these curves serve as an informative upper bound on the performance. It is observed that even a 2-stage reduced-rank filter outperforms the Rake at all SNRs and only a small number of stages of the MSNWF are needed in order to achieve near full-rank MMSE performance over a practical range of SNRs.

Figures 6b and 7b display similar plots, but for the edge of cell scenario. In this case, there are 4 effective channels at the receiver, because we sampled the received signal at twice the chip-rate at each antenna. It can be shown that the two-polyphase channels created from either antenna are nearly linearly dependent in the case of a sparse multipath channel as in our simulations. The dimension of the full space is 228, which makes the full rank calculations very cumbersome. Amazingly, the MSE for MSNWF still goes down very steeply with rank and achieves the full-rank value for subspace dimension of only 8 or so. Compared to the PC and CS methods, this is a huge difference in effective rank reduction. In the BER plots of Figure 7b, the bit error is calculated for the soft handoff mode. With perfect channel estimation, the MSNWF can achieve error rates similar to the full-rank MMSE over practical SNR range after stopping at stage as low as 5!

6. ADAPTIVE EQUALIZATION

Next, we use the class of training-based adaptive algorithms presented by Honig and Goldstein in [23] to simulate the performance of MSNWF when the channel is unknown. Although the MMSE equalizer described in this paper estimates the chip-rate multiuser synchronous sum signal, it is not possible to train the equalizer on this signal as that would require

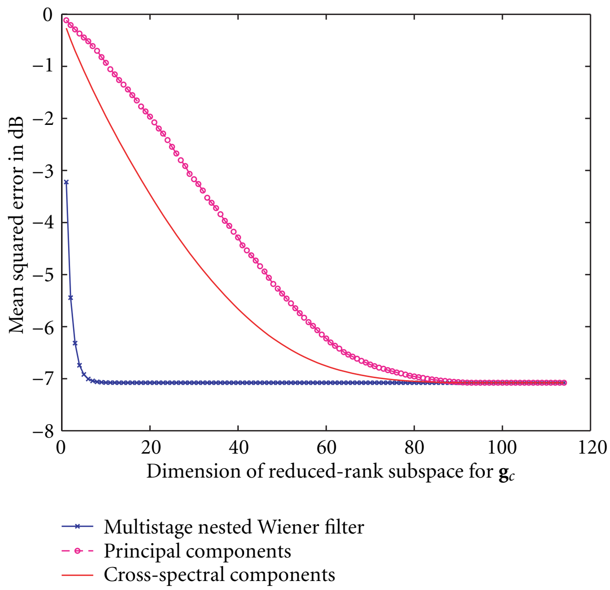

(a) One base station.

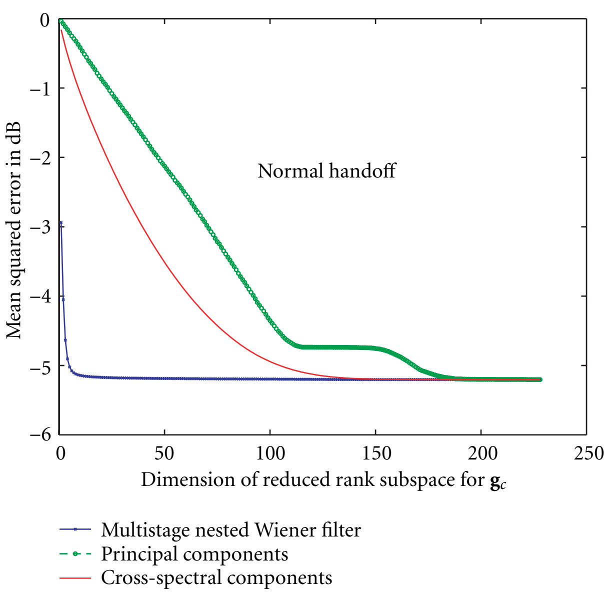

(b) Two base stations.

FIGURE 6: MSE versus rank of reduced dimension subspace, known channels, SNR = 10 dB.

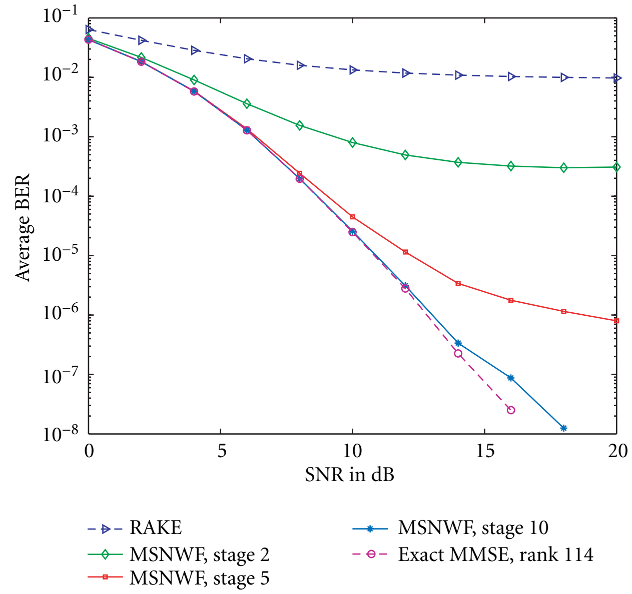

(a) One base station.

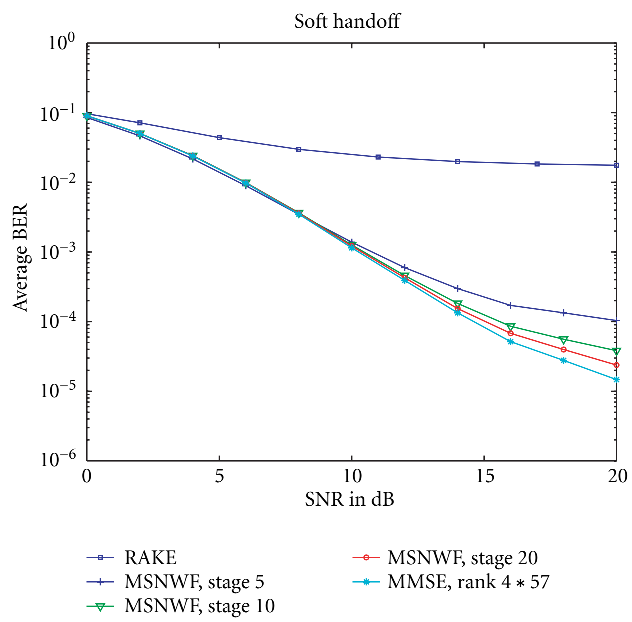

(b) Two base stations.

FIGURE 7: BER for different chip-level equalizers for CDMA downlink, known channels.

the knowledge of number of active users, all of the active channel codes and the transmitted symbols. Instead, we use the pilot channel of CDMA downlink, which has a known code and known symbols. For DS-CDMA with orthogonal spreading codes, the chip-level MMSE equalizer restores the synchronous sum signal transmitted by the base station, so the MMSE equalizer is identical for all channels within a multiplicative constant and the common pilot code can be used to train for any other channel code [5]. Our approach is to train off the pilot symbols by using directly the following relations (cf. Figure 1):

(i) Chip-level equalization

$$z[n] = \mathbf{g}_c^H \mathbf{x}[n], \quad \mathbf{x}[n] = \begin{bmatrix} x[n] \\ x[n-1] \\ \vdots \\ x[n-N_g+1] \end{bmatrix}. \tag{18}$$

(ii) Despreading

$$\begin{aligned}\hat{b}_1[m] &= \sum_{i=0}^{N_c-1} z[n+i]c_{bs}^*[n+i]c_1^*[i], \quad n = mN_c + D_c \\ &= \sum_{i=0}^{N_c-1} \left\{ \mathbf{g}_c^H \mathbf{x}[n+i] \right\} c_{bs}^*[n+i] \\ &= \mathbf{g}_c^H \left\{ \sum_{i=1}^{N_c} \mathbf{x}[n+i]c_{bs}^*[n+i] \right\} \\ &\equiv \mathbf{g}_c^H \mathbf{C}_1^H[m]\tilde{\mathbf{x}}[m] = \mathbf{g}_c^H \mathbf{y}[m],\end{aligned} \tag{19}$$

where

$$\tilde{\mathbf{x}}[m] = \begin{bmatrix} x[n+N_c-1] \\ \vdots \\ x[n] \\ \vdots \\ x[n-N_g+1] \end{bmatrix},$$

$$\mathbf{C}_1[m] = \begin{bmatrix} c_{bs}[mN_c+N_c-1] & 0 & \cdots & \cdots \\ \vdots & \ddots & \ddots & \vdots \\ c_{bs}[mN_c] & c_{bs}[mN_c+1] & \cdots & c_{bs}[mN_c+N_g-1] \\ \ddots & \ddots & \ddots & \vdots \\ 0 & 0 & \cdots & c_{bs}[mN_c] \end{bmatrix} \tag{20}$$

assuming that $N_g \leq N_c$.

Thus we convolve the received chip-sequence with the pilot channel code (which is all 1's) times the appropriate portion of the base station scrambling code, and then train the equalizer on the pilot symbols. This is equivalent to first equalizing and then despreading due to the commutativity of convolution. We use a *block-adaptive* training-based algorithm that implements the lattice-type MSNWF of Figure 4. The algorithm is given in Algorithm 2. We also find the full-rank Wiener solutions, using least mean squares and recursive least squares algorithms for purposes of comparison in the simulations.

First, we simulate the single base station scenario, where the dimension of the full-rank solution is 114 as described before. Figure 8 plots the output SINR for different chip-level equalizers versus time in symbols, at a fixed SNR. The output SINR is calculated using the formula derived by Krauss in [27]. The MSNWF after stages 5 and 10 yields very good performance with low sample-support. The convergence rate is similar to that of a full-rank RLS, which even asymptotically, does not beat the MSNWF of rank only 10! The LMS algorithm converges much slower and to a lower SINR. For the two-base station case, we implement soft handoff. The asymptotic SINR is almost 3 dB lower for all the equalizers due to the added interference from the MAI of the second base station. But the convergence speed of low-rank MSNWF is still impressive.

Block size = N_t symbols.

- *Initialization*:
  $\mathbf{d_0} = \mathbf{b}$ where $\mathbf{b}$ is the length N_t vector of the pilot symbols, and $\mathbf{Y}_0 = [\mathbf{y}[1], \ldots, \mathbf{y}[N_t]]$, $\mathbf{y}[m] = \mathbf{C}_1^H[m]\tilde{\mathbf{x}}[m]$.
- *Forward recursion*:
  For $k = 1, 2, \ldots, D$,

$$\begin{aligned}\mathbf{c}_k &= \mathbf{Y}_{k-1}\mathbf{d}_{k-1}^H, \\ \delta_k &= \|\mathbf{c}_k\|, \\ \mathbf{p}_k &= \mathbf{c}_k/\delta_k, \\ \mathbf{d}_k &= \mathbf{p}_k^H \mathbf{Y}_{k-1}, \\ \mathbf{Y}_k &= \mathbf{Y}_{k-1} - \mathbf{p}_k \mathbf{d}_k,\end{aligned}$$

- *Backward recursion*:
  $\boldsymbol{\epsilon}_D = \mathbf{d}_D$,
  For $k = D, D-1, \ldots, 1$ Do

$$\begin{aligned}w_k &= (\epsilon_k \mathbf{d}_{k-1}^H)/\|\boldsymbol{\epsilon}_k\|^2 = \delta_k/\|\boldsymbol{\epsilon}_k\|^2, \\ \boldsymbol{\epsilon}_{k-1} &= \mathbf{d}_{k-1} - w_k \boldsymbol{\epsilon}_k\end{aligned}$$

Algorithm 2: Structured lattice MSNWF algorithm for the CDMA forward link.

The output SINR is plotted versus the rank of the reduced dimension subspace, D, in Figure 9 at two different SNRs. For comparison, the SINR output for an "ideal" MSNWF, that is, with perfect channel estimation, is included. At a low SNR of 0 dB, the SINR after 200 symbols for the adaptive MSNWF shows a distinct peak at a dimension of only 3! At 10 dB SNR, the peak is less prominent, but the SINR output goes down after stage 8 or so. This can be explained as the "penalty" for learning the channels, that is, in the presence of significant noise, the lower rank MSNWF trades off a bias in the symbol estimate for a lower variance by working in a lower dimensional space so as to pass less noise. As the signal power increases, the higher-dimensional filters yield better approximation to the full-rank solution, as the lower rank filters do not have adequate degrees of freedom to suppress MAI and ISI.

The BER curves in Figure 10 illustrate the performance of these equalizers after training with 200 symbols in the single base station case, and 300 symbols in the multiple base stations case. At low SNRs, the BER for MSNWF stage 5 is actually slightly lower than the BER for stage 10 or 15, as expected from the SINR graphs of Figure 9.

It is noteworthy that over a practical SNR range, in this adaptive implementation, the stage 5 MSNWF does better or almost as good as full-rank RLS! Another remarkable fact is that the pilot channel had the same power as all the traffic channels, implying that the MSNWF reduced-rank adaptation does not require a strong pilot signal for fast convergence. Obviously, the rate of convergence would increase if the amplitude of the pilot channel was made higher than the traffic channels, and the BER floor would improve for the adaptive equalizers.

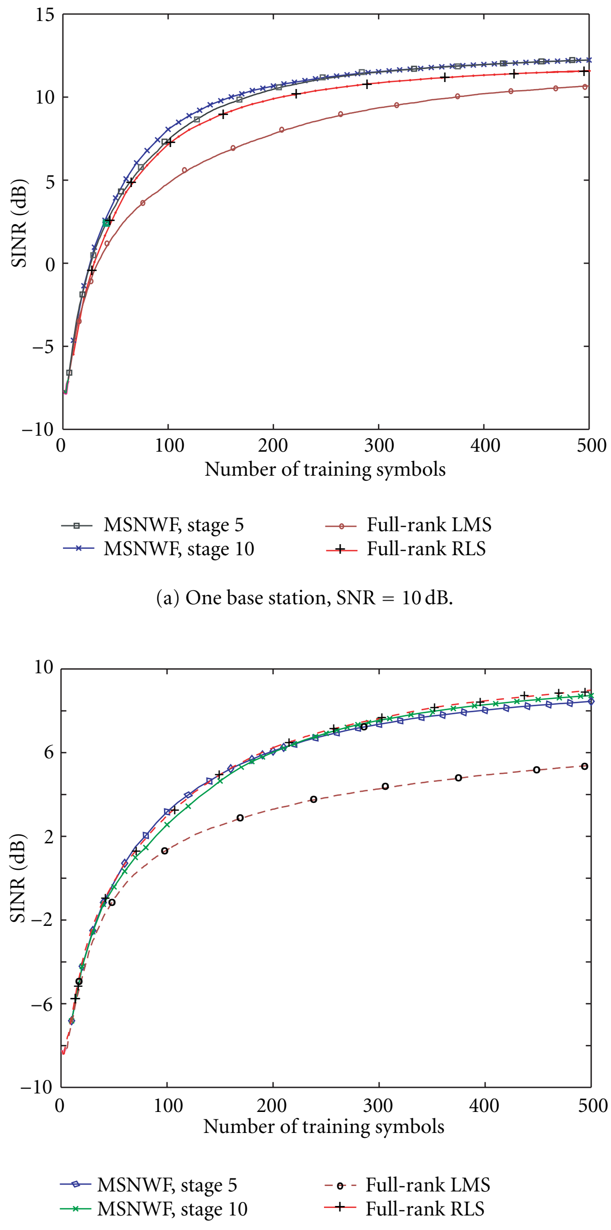

(a) One base station, SNR = 10 dB.

(b) Two base stations, SNR = 10 dB, soft handoff.

Figure 8: Output SINR versus time for adaptive chip-level equalizers for CDMA downlink.

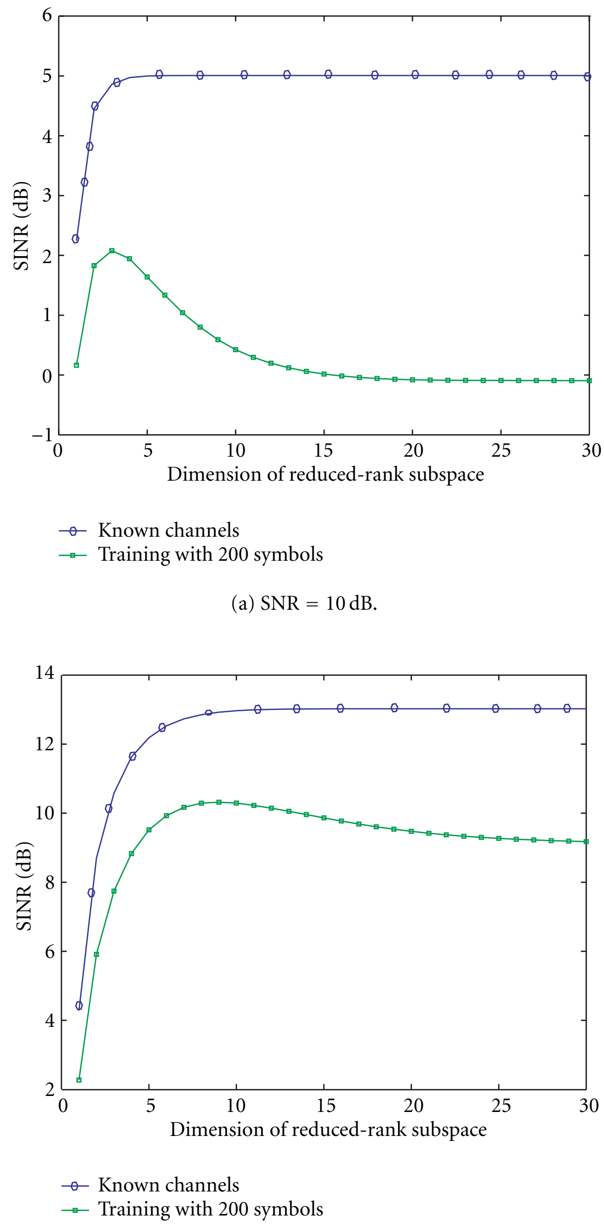

(a) SNR = 10 dB.

(b) SNR = 10 dB.

Figure 9: SINR of MSNWF versus dimension of reduced-rank subspace, 1 base station.

7. STRUCTURED EQUALIZER IN SPARSE MULTIPATH

For high-speed CDMA, typically the vector of multipath channel coefficients is sparse, but the chip-rate linear equalizers will not be sparse in general. Under certain conditions, the overall channel coefficients lie in a subspace associated with the pulse shaping filter convolution matrix. A semi-blind direct equalization approach that utilizes this structure to impose a penalty on nonblind equalizers was presented in [31], and compared to nonblind MMSE equalizers for indoor channels. For wideband CDMA, additional benefits may be obtained by realizing that, due to the sparse nature of the multipath arrivals, the total channel vector lies in a subspace spanned by only a few columns of the pulse shaping convolution matrix [10]. If we project the full-rank chip-level MMSE equalizer onto this much lower-rank subspace, the equalizer should converge much faster.

It was shown in Section 3 that the channel cross-correlation vector is given by

$$\mathbf{r}_{dx} = \mathcal{H}\boldsymbol{\delta}_{D_c}. \tag{21}$$

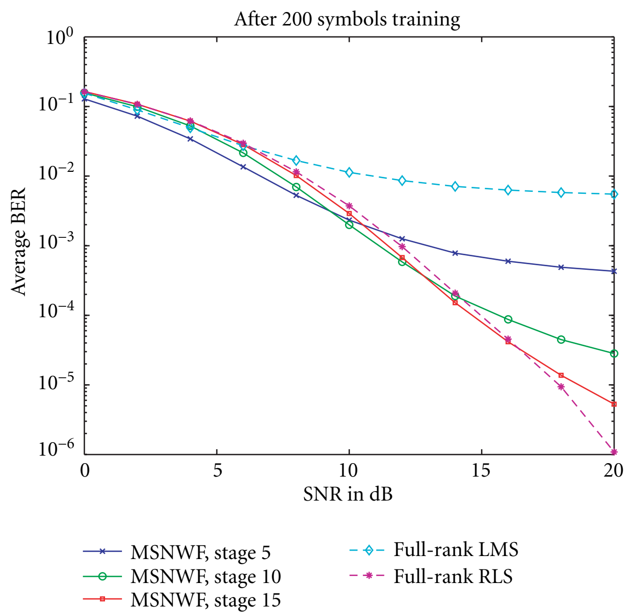

(a) One base station.

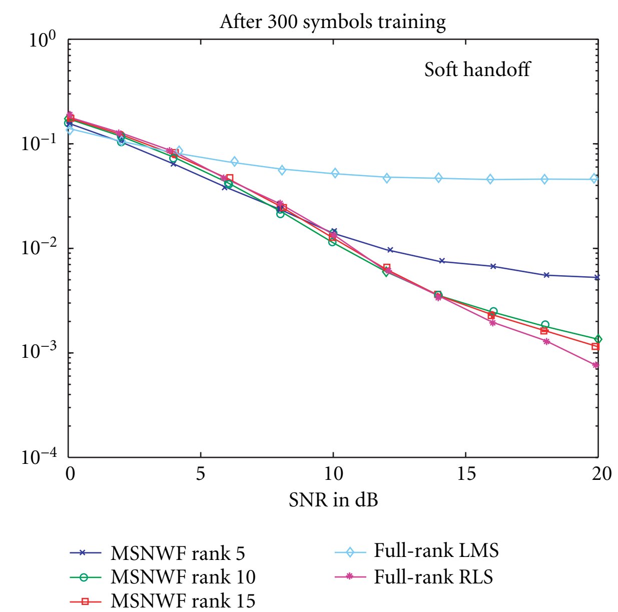

(b) Two base stations.

FIGURE 10: BER for adaptive chip-level equalizers for CDMA downlink.

If we restrict ourselves to the following two conditions:

(1) $N_g \geq L$, and
(2) $N_g - 1 \geq D_c \geq L - 1$,

then it can be easily seen that $\mathbf{r}_{dx}$ now contains all the elements of the channel impulse response. In particular, if we choose $N_g = L$ and $D_c = L - 1$, we get

$$\mathbf{r}_{dx} = \begin{bmatrix} & \tilde{\mathbf{I}} \\ \tilde{\mathbf{I}} & \end{bmatrix} \begin{bmatrix} \mathbf{h}_1 \\ \mathbf{h}_2 \end{bmatrix}, \quad \tilde{\mathbf{I}} = \begin{bmatrix} 0 & \cdots & 1 \\ & & \cdot \\ & \cdot & \\ \cdot & & \\ 1 & \cdots & 0 \end{bmatrix}. \tag{22}$$

The impulse response for the channel between the transmitter and the ith antenna at the receiver is given by (cf. (1))

$$h_i(t) = \sum_{k=0}^{N_m-1} h_{c_i}[k] p_{rc}(t - \tau_k), \quad i = 1, 2. \tag{23}$$

If we sample at chip rate and assume a high enough chip rate so that the multipath delays are integer multiples of the chip period T_c (we will relax this assumption shortly), we can write the channel vectors in (22) as

$$\mathbf{h}_i = \mathbf{G}\mathbf{h}_{c_i}, \quad i = 1, 2, \tag{24}$$

where $\mathbf{G}$ is the convolution matrix corresponding to the chip pulse waveform, and $\mathbf{h}_{c_i}$ is a sparse vector containing the multipath coefficients. In this case, the vector channel $\mathbf{h}_i$ lies in a subspace spanned by only a few columns of $\mathbf{G}$ and we can simplify (21) as

$$\mathbf{r}_{dx} = \begin{bmatrix} & \mathbf{G}_p \\ \mathbf{G}_p & \end{bmatrix} \begin{bmatrix} \mathbf{h}_{p_1} \\ \mathbf{h}_{p_2} \end{bmatrix} = \mathcal{G}\mathbf{h}_p, \tag{25}$$

where $\mathbf{G}_p$ contains only the L_c columns of $\tilde{\mathbf{I}}\mathbf{G}$ corresponding to the L_c dominant multipath arrivals, and $\mathbf{h}_p$ is the vector of corresponding complex gains, that is, $\mathbf{h}_p$ consists of only nonzero elements of $\mathbf{h}_c$.

Thus the chip-level MMSE equalizer has the form

$$\mathbf{g}_c = \mathbf{R}_{xx}^{-1}\mathbf{r}_{dx} = \mathbf{R}_{xx}^{-1}\mathcal{G}\mathbf{h}_p. \tag{26}$$

This structure due to the sparse multipath channel can be utilized to increase the convergence speed of adaptive MMSE equalizers, if an estimate of the multipath arrival times τ_k, $k = 1, \ldots, L_c$ is available at the receiver. We can then project the observed data vector onto a rank $2L_c \ll 2L$ subspace by taking

$$\mathbf{y}_r[m] = \mathcal{G}^H \mathbf{R}_{xx}^{-1} \mathbf{C}_j^H[m] \tilde{\mathbf{x}}[m]. \tag{27}$$

This would also require estimation of the chip-level covariance matrix. We refer to the MMSE equalizer residing in this low-rank subspace as the "structured projected" equalizer, denoted by $\mathbf{g}_r$. Then the estimate of the desired user's symbol is given by

$$\hat{b}_j[m] = \mathbf{g}_r^H \mathbf{y}_r[m] \equiv \hat{\mathbf{h}}_p^H \mathbf{y}_r[m]. \tag{28}$$

7.1. Chip-level whitening with multistage nested Wiener filter

Direct inversion of $\mathbf{R}_{xx}$ in (27) can be avoided using the MSNWF to obtain a reduced-rank solution to

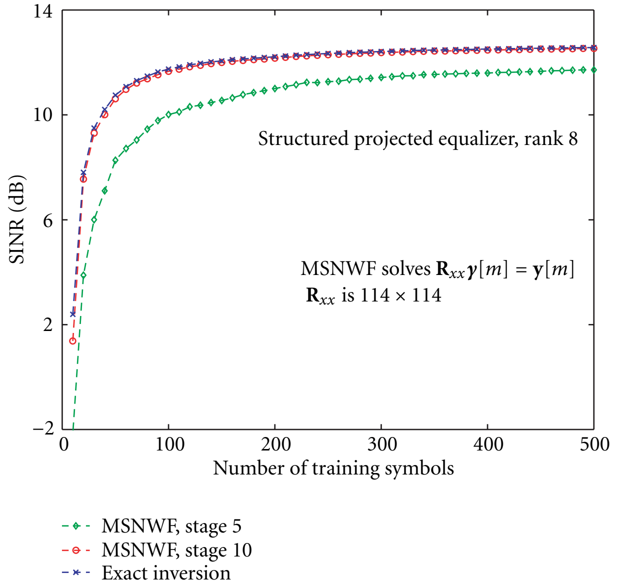

Figure 11: Application of MSNWF to covariance matrix inversion, SNR = 10 dB.

$$\mathbf{R}_{xx}\boldsymbol{\gamma}[m] \approx \mathbf{y}[m]. \qquad (29)$$

Then $\hat{\mathbf{y}}_r[m] = \mathcal{G}^H\boldsymbol{\gamma}[m]$ is an approximation to the projected data-vector.

The efficacy of the MSNWF is illustrated in Figure 11, which plots the output SINRs of 3 structured equalizers, the only difference is the use of 5 or 10 stages of the MSNWF to get approximate solution $\hat{\mathbf{y}}_r[m]$ or direct inversion of $\mathbf{R}_{xx}$ to obtain exact solution $\mathbf{y}_r[m]$. The dimension of $\mathbf{R}_{xx}$ is 114×114, so its inversion is prohibitively expensive, but only 10 stages of MSNWF is sufficient to give the same SINR overall.

7.2. Generalized arrival times

When the multipath arrival times are not exact multiples of the chip period, (24) is only an approximate relation. In this case we form the basis vector matrix $\mathbf{G}^{(\nu)}$ by sampling the chip-pulse shaping filter at rate T_c/ν. The approximation error can be made arbitrarily small by increasing ν.

The basis matrix $\mathbf{G}_p$ is now formed by taking $(\nu+1)$ consecutive columns of $\tilde{\mathbf{I}}\mathbf{G}^{(\nu)}$ for each multipath arrival, corresponding to $\nu\lfloor \tau_k/T_c \rfloor, \dots, \nu\lceil \tau_k/T_c \rceil$. Maximum rank of structured projected equalizer is now $2L_c(\nu + 1)$. Note that our scheme does not require any increase in the sampling rate of the received signal.

7.3. Delay estimation

The structured projected equalizer requires estimate of the multipath delays, but no knowledge of the multipath coefficients is needed. The multipath delays will change relatively slowly as compared to the complex gains even in a time-varying situation. The use of multiple antennas at the receiver enhances the quality of the delay estimates since the arrival times are the same at both antennas (the propagation

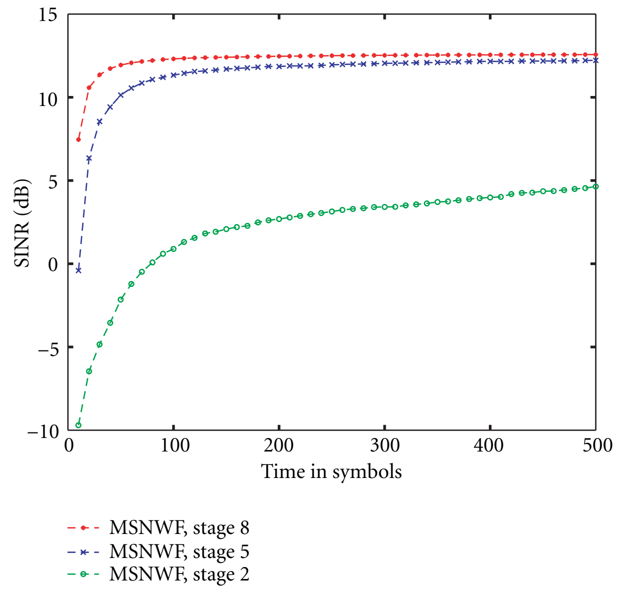

(a) Structured projected equalizers.

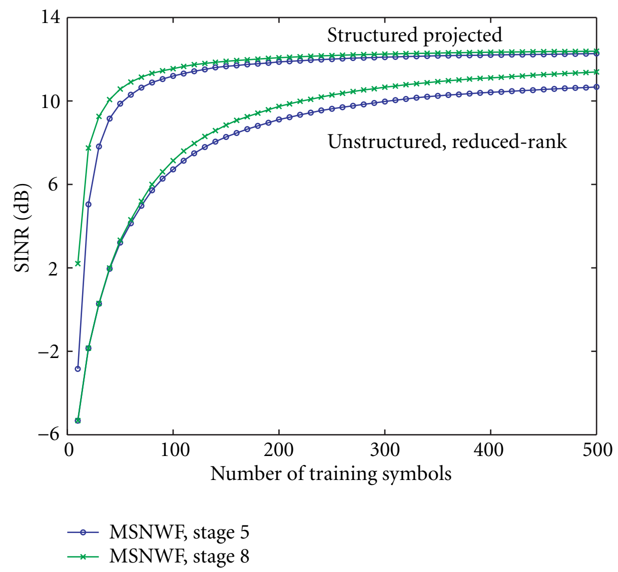

(b) Comparison of structured projected and unstructured equalizers.

Figure 12: SINR convergence for chip-level equalizers using MSNWF, arrivals at exact chip-periods, SNR = 10 dB.

delay between two antennas at the mobile is negligible for a given multipath). Typically in CDMA mobile receivers, a serial or block serial search is performed over a very short interval where the channels are assumed to be unchanging (perhaps over 512 chips), where the received sequence is correlated with the base station long code. These short coherent correlations are combined in energy to obtain the delay estimates. This approach yields fast, accurate delay estimates. If the estimate is deemed to be not enough reliable, 2 or

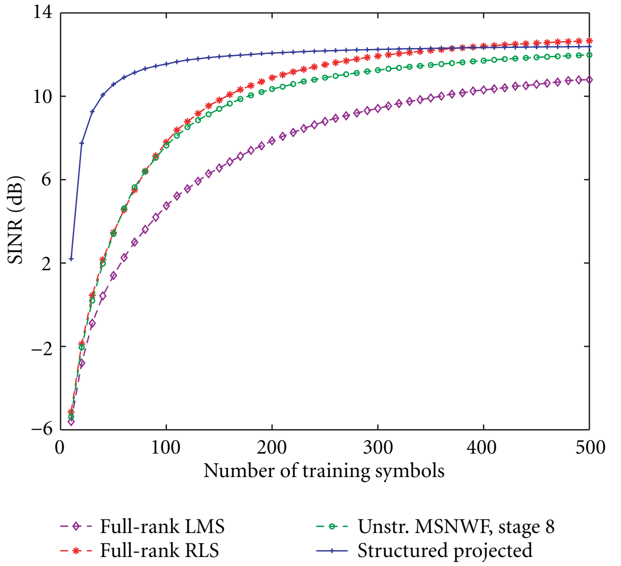

Figure 13: SINR versus time for different equalizers, arrivals at exact chip-periods, SNR = 10 dB.

3 columns of $\tilde{\mathbf{I}}\mathbf{G}$ centered on the doubtful estimate may be taken to form $\mathbf{G}_p$.

8. RESULTS

Figure 12a shows the output SINR vs. time (in symbols) at a fixed SNR of 10 dB for “structured projected” chip-level equalizers, for channels simulated as described in Section 5, that is, the arrival times are at exact multiples of the chip-period T_c. We assume that the receiver has already formed estimates of the multipath arrival times. After the projection via (27), we use different stages of the MSNWF algorithm. The stage 2 MSNWF does not perform very well, but the convergence rate for stages 5 and 8 (maximum) is very good, as expected.

Figure 12b compares the SINR convergence speed of training-based unstructured chip-level equalizers and the structured projected equalizers, all of which use a MSNWF solution. It is clear that the structured projected equalizers exploit the structure in the sparse channels to yield a much superior performance. The structured projected equalizer is compared to full-rank RLS and LMS convergence in Figure 13. After training with 100 symbols there is approximately 5 dB difference in output SINRs of the structured projected MMSE equalizer and an unstructured MSNWF solution of rank 10 and full-rank RLS.

Next, we simulate frequency-selective channels where the first multipath arrival is at 0, and the other three are uniformly distributed within 10 μs, with the only constraint being that the multipath delays are spaced at least one chip-period apart. Figure 14a shows the SINR plot after various stages of the MSNWF where the basis vectors are formed by sampling the pulse-shaping filter at rate T_c. In this case the structured projected equalizers are of dimension 14, as we form $\mathbf{G}_p$ by taking two consecutive columns of $\tilde{\mathbf{I}}\mathbf{G}$ corresponding to each multipath arrival that is in between two chip-periods. We see that 8 stages of the MSNWF are sufficient but there is a loss of about 2 dB in asymptotic SINR compared to Figure 12a due to the arrival times not being at exact chip periods.

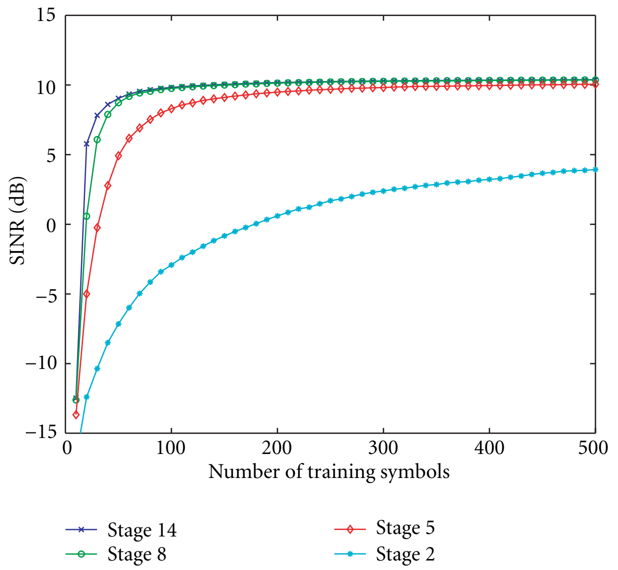

(a) Basis vectors formed by sampling at T_c.

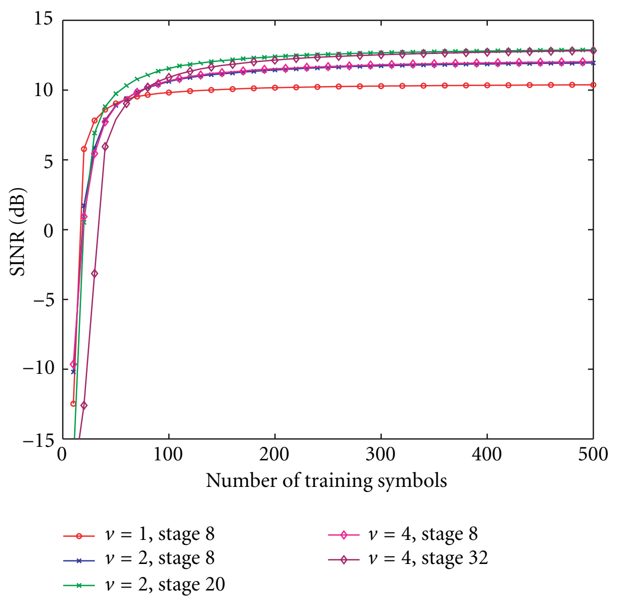

(b) Basis vectors formed by sampling at T_c/ν.

Figure 14: SINR convergence for chip-level equalizers using MSNWF, random arrivals, SNR = 10 dB.

Figure 14b shows the SINR plot where the basis vectors are formed by sampling the pulse-shaping filter at rate T_c, $T_c/2$, and $T_c/4$. The SINR loss compared to Figure 12a is

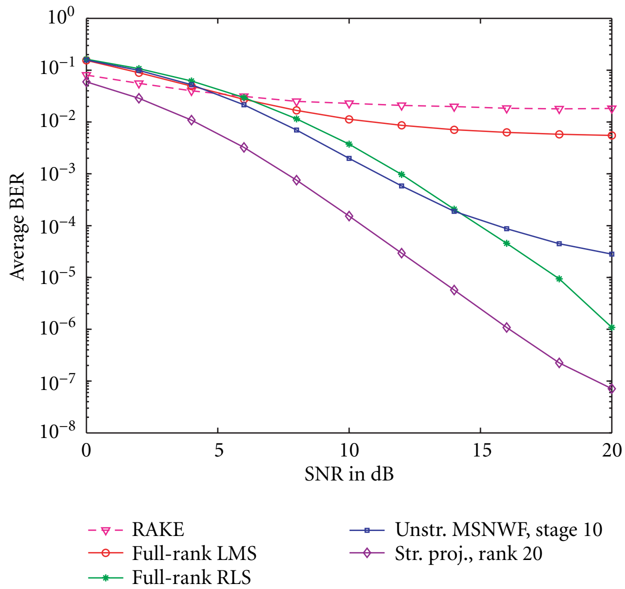

Figure 15: Bit error rates graph, random arrival times.

recouped if we oversample by a factor of 2 and perform full-rank equalization (which is now rank 20). At $T_c/4$ the convergence goes down due to the increased dimension of the filter (which is now 32) but there is no improvement in asymptotic SINR.

We plot the bit error rate graphs of the structured projected equalizer where the pulse-shaping filter is sampled at rate $T_c/2$, compare it with the full-rank RLS, and reduced-rank unstructured equalizer curves in Figure 15. The multipath delays are randomly distributed within 10 μs. The structured projected equalizer (of rank 20) exhibits significantly lower bit errors for all SNRs.

9. CONCLUSIONS

We presented reduced-rank chip-level MMSE equalizers for the CDMA downlink with frequency-selective multipath based on the multistage nested Wiener filter, for known channel case and also for training-based adaptation. The performance for the single base station case, and for the edge-of-cell scenario with soft handoff are very satisfactory. The convergence rate for MSNWF operating in a very low-rank subspace was significantly better than LMS, and somewhat better than RLS. The BER performance showed improvement over the full-rank methods for practical SNR range. This excellent performance is achieved at a computational complexity in between LMS and RLS due to lattice-type structure that allows block-adaptive implementation through simple filtering operations.

We also developed a structured MMSE equalizer that utilizes the estimate of the multipath arrival times and sparse nature of the multipath channel to substantially reduce the number of parameters that need to be adapted. The convergence rate for this projected MMSE equalizer was significantly better than unstructured MSNWF operating in a subspace of similar rank. The bit error rate performance of this structured MMSE equalizer was shown to be superior to full-rank RLS and reduced-rank unstructured MMSE equalizer over a wide SNR range.

ACKNOWLEDGMENT

This research was supported by the Air Force Office of Scientific Research under grant No. F49620-00-1-0127 and by Texas Instruments' DSP University Research Program.

REFERENCES

[1] J. G. Proakis, *Digital Communications*, McGraw-Hill, New York, NY, USA, 3rd edition, 1995.

[2] T. P. Krauss, M. D. Zoltowski, and G. Leus, "Simple MMSE equalizers for CDMA downlink to restore chip sequence: comparison to zero-forcing and rake," in *Proc. IEEE Int. Conf. Acoustics, Speech, Signal Processing*, pp. 2865–2868, Istanbul, Turkey, June 2000.

[3] W. van Etten, "Maximum likelihood receiver for multiple channel transmission systems," *IEEE Trans. Communications*, vol. 24, no. 2, pp. 276–283, 1976.

[4] S. Werner and J. Lilleberg, "Downlink channel decorrelation in CDMA systems with long codes," in *Proc. IEEE Int. Conf. on Communications*, Vancouver, Canada, June 1999.

[5] C. D. Frank and E. Visotsky, "Adaptive interference suppression for direct-sequence CDMA systems with long spreading codes," in *Proc. 36th Allerton Conf. on Communication, Control, and Computing*, Monticello, Ill, USA, September 1998.

[6] A. Klein, "Data detection algorithms specially designed for the downlink of CDMA mobile radio systems," in *Proc. IEEE Vehicular Technology Conference*, vol. 1, pp. 203–207, Phoenix, Ariz, USA, May 1997.

[7] I. Ghauri and D. T. M. Slock, "Linear receivers for the DS-CDMA downlink exploiting orthogonality of spreading sequences," in *Proc. 32nd Asilomar Conf. on Signals, Systems, and Computers*, Pacific Grove, Calif, USA, November 1998.

[8] K. Hooli, M. Latva-aho, and M. Juntti, "Multiple access interference suppression with linear chip equalizers in WCDMA downlink receivers," in *Proc. IEEE Global Telecommunications Conf.*, vol. 1, pp. 467–471, Rio de Janero, Brazil, December 1999.

[9] M. D. Zoltowski and T. P. Krauss, "Two-channel zero forcing equalization on CDMA forward link: Trade-offs between multi-user access interference and diversity gains," in *Proc. 33rd Asilomar Conf. on Signals, Systems and Computing*, Pacific Grove, Calif, USA, October 1998.

[10] I. Ghauri and D. T. M. Slock, "Structured estimation of sparse channels in quasi-synchronous DS-CDMA," in *Proc. IEEE Int. Conf. Acoustics, Speech, Signal Processing*, Istanbul, Turkey, June 2000.

[11] M. J. Heikkila, P. Komulainen, and J. Lilleberg, "Interference suppression in CDMA downlink through adaptive channel equalization," in *Proc. Vehicular Technology Conference*, vol. 2 of *Gateway to 21st Century Communications*, pp. 978–982, Amsterdam, Netherlands, September 1999.

[12] P. Komulainen and M. J. Heikkila, "Adaptive channel equalization based on chip separation for CDMA downlink," in

Proc. IEEE Int. Symp. Personal, Indoor and Mobile Radio Communications, September 1999.

[13] K. Hooli, M. Latva-aho, and M. Juntti, "Performance evaluation of adaptive chip-level channel equalizers in WCDMA downlink," in *IEEE Int. Conf. on Communications*, Helsinki, Finland, June 2001.

[14] K. Hooli, M. Latva-aho, and M. Juntti, "Novel adaptive channel equalizer for WCDMA downlink," in *Proc. COST 262 Workshop*, pp. 7–11, Ulm, Germany, January 2001.

[15] J. S. Goldstein, I. S. Reed, and L. L. Scharf, "A multistage representation of the Wiener filter based on orthogonal projections," *IEEE Transactions on Information Theory*, vol. 44, no. 7, pp. 2943–2959, 1998.

[16] J. S. Goldstein and I. S. Reed, "A new method of Wiener filtering and its application to interference mitigation for communications," in *Proc. IEEE Military Communications Conference*, Monterey, Calif, USA, November 1997.

[17] J. S. Goldstein, J. R. Guerci, and I. S. Reed, "An optimal generalized theory of signal representation," in *Proc. IEEE Int. Conf. Acoustics, Speech, Signal Processing*, Phoenix, Ariz, USA, March 1999.

[18] X. Wang and H. V. Poor, "Blind multiuser detection: A subspace approach," *IEEE Transactions on Information Theory*, vol. 44, no. 2, pp. 677–690, 1998.

[19] J. S. Goldstein and I. S. Reed, "Reduced-rank adaptive filtering," *IEEE Trans. Signal Processing*, vol. 45, no. 2, pp. 492–496, 1997.

[20] D. A. Pados and S. N. Batalama, "Low-complexity blind detection of DS/CDMA signals: Auxilliary-vector receivers," *IEEE Trans. Communications*, vol. 45, no. 12, pp. 1586–1594, 1997.

[21] D. A. Pados, F. J. Lombardo, and S. N. Batalama, "Auxiliary-vector filters and adaptive steering for DS/CDMA single-user detection," *IEEE Trans. Vehicular Technology*, vol. 48, no. 6, pp. 1831–1839, 1999.

[22] A. Kansal, S. N. Batalama, and D. A. Pados, "Adaptive maximum SINR rake filtering for DS-CDMA multipath fading channels," *IEEE Journal on Selected Areas in Communications*, vol. 16, no. 9, pp. 1831–1839, 1998.

[23] M. L. Honig and J. S. Goldstein, "Adaptive reduced-rank residual correlation algorithms for DS-CDMA interference suppression," in *Proc. 32nd Asilomar Conf. on Signals, Systems, and Computing*, Pacific Grove, Calif, USA, November 1998.

[24] M. L. Honig and W. Xiao, "Large system performance of reduced-rank linear interference supression for DS-CDMA," in *Proc. Allerton Conf. on Communication, Control, and Computing*, UIUC, October 1999.

[25] W. L. Myrick, M. D. Zoltowski, and J. S. Goldstein, "Anti-jam space-time preprocessor for GPS based on multistage nested Wiener filter," in *Proc. IEEE Military Communications Conference*, Atlantic City, NJ, USA, October 1999.

[26] W. L. Myrick, M. D. Zoltowski, and J. S. Goldstein, "Low-sample performance of reduced-rank power minimization based jammer suppression for GPS," in *IEEE Sixth International Symposium on Spread Spectrum Techniques & Applications*, pp. 93–97, Parsippany, NJ, USA, September 2000.

[27] T. P. Krauss and M. D. Zoltowski, "MMSE equalization under conditions of soft hand-off," in *IEEE Sixth International Symposium on Spread Spectrum Techniques & Applications*, pp. 540–544, NJIT, Parsippany, NJ, USA, September 2000.

[28] T. P. Krauss, W. J. Hillery, and M. D. Zoltowski, "MMSE equalization for forward link in 3G CDMA: symbol-level versus chip-level," in *Proc. 10th IEEE Workshop on Statistical Signal and Array Processing*, pp. 18–22, Pocono Manor, Pa, USA, August 2000.

[29] M. Joham and M. D. Zoltowski, "Interpretation of the multistage nested Wiener filter in the Krylov subspace framework," Tech. Rep. TR-ECE-00-51, Purdue University, West Lafayette, Ind, USA, November 2000.

[30] D. Ricks and J. S. Goldstein, "Efficient architectures for implementing adaptive algorithms," in *Allerton Antenna Arrays Symp.*, UIUC, September 2000.

[31] B. C. Ng, D. Gesbert, and A. Paulraj, "A semi-blind approach to structured channel equalization," in *Proc. IEEE Int. Conf. Acoustics, Speech, Signal Processing*, Seattle, Wash, USA, May 1998.

Samina Chowdhury was born in Dhaka, Bangladesh in December 1971. She received her B.S. degree in electrical and electronic engineering from Bangladesh University of Engineering and Technology, Dhaka, Bangladesh in June 1996 with the top position in her class. She was employed as a Lecturer in the Electrical Engineering Department of BUET from October 1996 to July 1997. She enrolled in the Ph.D. program in electrical and computer engineering at Purdue University, West Lafayette, Indiana, in August 1997. She completed her Ph.D. in December 2001 under supervision of Professor Michael D. Zoltowski. Her research interests include mobile cellular communications, space-time processing, reduced-rank linear processing, and physical layer system design for wireless communications.

Michael D. Zoltowski was born in Philadelphia, PA, on August 12, 1960. He received both the B.S. and M.S. degrees in electrical engineering with highest honors from Drexel University in 1983 and the Ph.D. in systems engineering from the University of Pennsylvania in 1986. In fall 1986, he joined the faculty of Purdue University where he currently holds the position of Professor of electrical and computer engineering. In this capacity, he was the recipient of the IEEE Outstanding Branch Counselor Award for 1989–1990 and the Ruth and Joel Spira Outstanding Teacher Award for 1990–1991. In August 2001, he was named a *University Faculty Scholar* by Purdue University. Dr. Zoltowski was the recipient of the IEEE Signal Processing Society's 1991 Paper Award (Statistical Signal and Array Processing Area), "The Fred Ellersick MILCOM Award for Best Paper in the Unclassified Technical Program" at the IEEE Military Communications (MILCOM '98) Conference, and a Best Paper Award at the *IEEE International Symposium on Spread Spectrum Techniques and Applications (ISSSTA 2000)*. He is also a corecipient of the IEEE Communications Society 2001 Leonard G. Abraham Prize Paper Award in the Field of Communications Systems. He is a contributing author to *Adaptive Radar Detection and Estimation*, Wiley, 1991, *Advances in Spectrum Analysis and Array Processing, Vol. III*, Prentice-Hall, 1994, and *CRC Handbook on Digital Signal Processing*, CRC Press, 1996. He has served as a consultant to the General Electric Company, and currently serves as a consultant to SAIC, Zenith, and ATLINKS. He has served as an associate editor for both the *IEEE Transactions on Signal Processing* and the *IEEE Communications Letters*. Within the IEEE Signal Processing Society, he has been a member of the Technical Committee for the Statistical Signal and Array Processing Area and the Technical Committee on DSP Education. Currently, he is a member of both the Technical Committee on Signal Processing for Communications (SPC) and the Technical Committee on Sensor and Multichannel (SAM) Processing. From 1998 to 2001, he was a member-at-large of the Board of Governors, and Secretary of the IEEE Signal Processing Society. He is a fellow of IEEE. His present research interests include space-time adaptive processing for all areas of mobile and wireless communications, GPS, and radar.

J. Scott Goldstein is an Assistant Vice-President at SAIC where he manages the Targeted Information Processing Solutions Division. He has over 17 years of experience in the fields of radar, sonar, communications, navigation, and imaging sensors. He is also an Adjunct Professor of electrical engineering at Virginia Tech, where he teaches courses on radar systems and signal processing. Dr. Goldstein is a Fellow of the IEEE, an Associate Vice-President of the IEEE Aerospace and Electronic Systems Society, a member of the IEEE Radar Systems Panel, and a member of the IEEE Fellow Selection Committee. His recent awards include the 2002 IEEE Fred Nathanson Radar Engineer of the Year Award and the 2001 IEE Clarke-Griffith Memorial Paper Award and Premium for the best paper in the IEE Proceedings—Radar, Sonar, and Navigation. Dr. Goldstein has authored or co-authored over 100 technical publications and is a member of Eta Kappa Nu, Tau Beta Pi, and Sigma Xi.